DOI: 10.1002/ejic.200600103

Synthesis, Structure, and Magnetic Properties of Hydroxo-Bridged Vanadium Oxalate $V_2O_2(OH)_2(C_2O_4)(H_2O)_2$

Sihai Yang,[a] Guobao Li,*[a] Shujian Tian,[a] Fuhui Liao,[a] and Jianhua Lin[a]

Keywords: Vanadium / Bridging ligands / Magnetic properties / Dimers / Oxalates

The reaction of V_2O_5 with $H_2C_2O_4{\cdot}2H_2O$ in the presence of H_3BO_3 under hydrothermal conditions has afforded $V_2O_2(OH)_2(C_2O_4)(H_2O)_2$ (**1**), which crystallizes in the triclinic system, space group $P\bar{1}$ with a = 5.2405(10) Å, b = 5.7340(11) Å, c = 7.1778(14) Å, α = 76.44(3)°, β = 69.37(3)°, γ = 75.37(3)°. The vanadium atoms in **1** form dimers by sharing edges consisting of μ-OH groups, and these dimers are connected further by oxalate ligands to form chains. The magnetic susceptibility data of **1** fit excellently with the Heisenberg dimer model in the temperature interval 2–300 K. Compound **1** is antiferromagnetic with a J value of –29.6 cm^{-1}.

Introduction

The oxalate ion $C_2O_4^{2-}$ shows a large variety of structural characteristics. It can act as a monodentate,[1] bidentate,[2] tridentate,[3] or tetradentate[4] donor ligand and can form chains,[5] layers,[6] or three-dimensional networks with metal centers.[7] In the presence of water molecules directly linked to the metal ions or weakly bonded to the framework,[5,8] abundant structural architectures in one-, two-, or three dimensions can be formed.[9] Moreover, the oxalate ion can mediate strong spin coupling between paramagnetic centers separated by more than 5 Å.[10] Thus, homo- and heterometallic systems involving oxalate ions (ox) as bridging ligands have been studied intensively in the search for new molecular-based magnets.[11–13] Because of the variable oxidation states of vanadium (V^{III}, V^{IV}, and V^{V}) and the coordination geometries of vanadium oxide polyhedra (tetrahedral, square pyramidal, trigonal bipyramidal, and octahedral),[14] many compounds containing both vanadium atoms and oxalate ions have been reported,[10,15–17] with different linkages between the vanadium atoms and the oxalate ions as shown in Figure 1, which result in different magnetic properties.[10,16,18–21] Recently, a new bonding mode for vanadium atoms and oxalate ions (Figure 1i) has been found in the compound $V_2O_2(OH)_2(C_2O_4)(H_2O)_2$ (**1**). The synthesis, structure and magnetic properties of **1** are reported below.

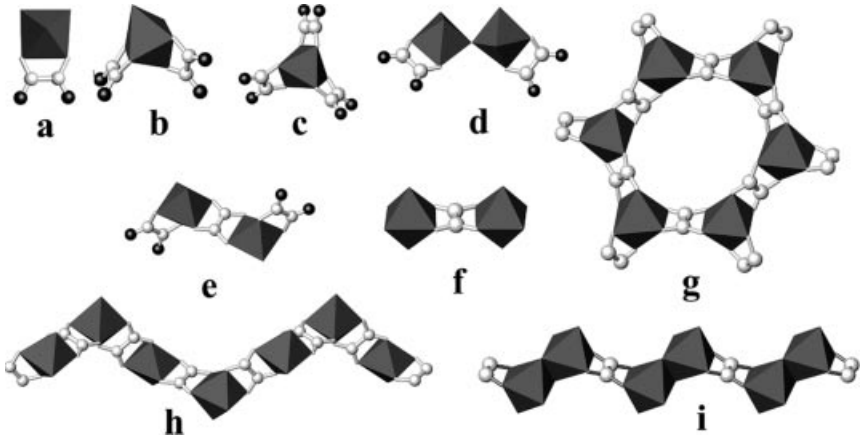

Figure 1. Different linkages between vanadium atoms and oxalate ions found in the literature. a) from ref.[19]; b) ref.[20]; c) ref.[10]; d) ref.[16]; e) ref.[21]; f) ref.[18]; g) inferred by ref.[10]; h) from ref.[21]; i) this work. C, white ball; O, black ball; VO_6, gray octahedron.

[a] Beijing National Laboratory for Molecular Sciences (BNLMS), State Key Laboratory of Rare Earth Materials Chemistry and Applications, College of Chemistry and Molecular Engineering, Peking University,
Beijing 100871, P. R. China
E-mail: liguobao@pku.edu.cn
Fax: +8610-62753541

Results and Discussion

Synthesis

The synthesis of compound **1** was performed in an aqueous solution of H_3BO_3 under hydrothermal conditions. Some experimental parameters, including the $V_2O_5/H_2C_2O_4$ molar ratio, were varied, but the resulting products remained the same. Finally, a $V_2O_5/H_2C_2O_4$ ratio of 1:14 was used. The formation of **1** was found to be sensitive to the presence of H_3BO_3. Compound **1** did not form when no H_3BO_3 was added to the mixture of V_2O_5, $H_2C_2O_4{\cdot}2H_2O$, and water. Although crystals of **1** formed from an aqueous solution, their solubility in pure water was low.

Crystal Structure

$V_2O_2(OH)_2(C_2O_4)(H_2O)_2$ is centrosymmetric in the triclinic system with the space group $P\bar{1}$, the center of inversion lies along the C–C bond of the bridging oxalato moiety, or on the common edge of two adjacent VO_6 octahedra. The asymmetric unit of **1** corresponds to half of the molecular formula, including one vanadium(IV) atom, half an oxalate ligand, one water molecule, one oxygen atom, and two half μ-OH groups. As shown in Figure 2, the vanadium(IV) atom binds to two oxygen atoms from one oxalate ligand, one oxygen atom from a water molecule, two oxygen atoms from the μ-OH groups, and one terminal oxo oxygen atom to form a distorted octahedron, a very common geometry in vanadium(IV) compounds.[10,16,18–21]

The VO_6 octahedra of **1** link together by sharing a common edge consisting of two μ-OH groups to form V_2O_{10} dimers; this type of link is rare in vanadium oxalate compounds. The typical ways to link oxalate ligands with VX_6 (X = O, Cl, F, and/or N) octahedra are shown in Figure 1.

The V_2O_{10} dimers are further linked by oxalate ligands to form chains (Figure 1i). The oxygen atoms of the μ-OH groups (O4) in one chain form hydrogen bonds with the oxygen atoms (O3) from the oxalate ions in the neighboring chain, which connects the chains into layers (Figure 3a). The water molecules coordinated to the vanadium atoms in one layer form two hydrogen bonds with the oxygen atoms

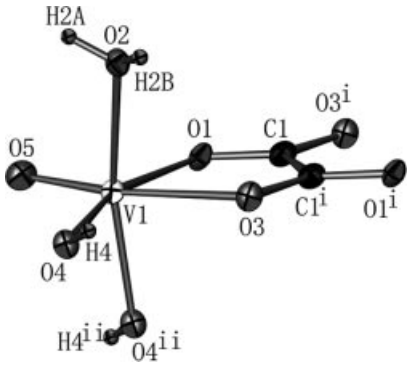

Figure 2. ORTEP drawing (at 30% probability) of the coordination environment of the vanadium atoms in $V_2O_2(OH)_2(C_2O_4)(H_2O)_2$. Symmetry codes: i) $1 - x, 1 - y, -z$; ii) $-x, 1 - y, 1 - z$.

of the μ-OH groups (O4) and the terminal oxo oxygen atoms (O5) in neighboring layers (Figure 3b). This results in the formation of a three dimensional net structure for **1**.

Vibrational Spectroscopy

The Fourier transform infrared (FTIR) spectrum of **1** exhibits two broad peaks centered at 3272 and 3041 cm^{-1}, mainly attributed to the symmetric and asymmetric stretching modes of water molecules and hydroxy groups. The signal for the bending mode of water expected at around 1600 cm^{-1} is overlapped by the intense oxalate band. The antisymmetric stretching mode of the oxalate ion appears at 1650 cm^{-1}. The peaks at 1355 cm^{-1} and 1311 cm^{-1} correspond to the symmetric stretching modes of the oxalate ion. The peak at around 979 cm^{-1} is assigned to the bending mode of the μ-OH group. The strong bands observed at around 771 and 731 cm^{-1} correspond to the in-plane deformation mode of the oxalate ion.

Thermal Stability

Thermogravimetric analysis shows that compound **1** is stable up to 200 °C and then undergoes decomposition to form a mixture of products with a maximum weight loss of

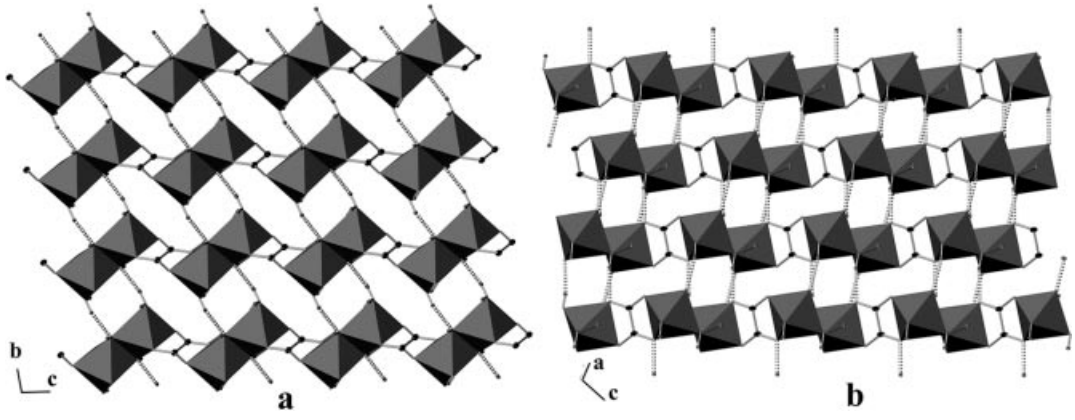

Figure 3. Packed structure of $V_2O_2(OH)_2(C_2O_4)(H_2O)_2$, showing hydrogen bonding.

40.0%. The mixture is then slowly oxidized to V_2O_5 with a total weight loss of 37.8% (calcd. 37.7%), as confirmed by X-ray diffraction data.

Magnetochemical Investigations

The magnetic properties of $V_2O_2(OH)_2(C_2O_4)(H_2O)_2$ are depicted in Figure 4. A near-perfect fit with the Heisenberg dimer model is attainable with the parameters listed in Table 3. A susceptibility maximum occurs near 50 K, and the compound exhibits Curie–Weiss paramagnetism at high temperatures. The compound is thus strongly antiferromagnetic with a J value of about –30 cm^{-1}, which is comparable to values for copper hydroxo-bridged dimers with antiferromagnetic coupling[22,23] and is larger than those for the (oxo)vanadium(IV) (d^1) oxalate-bridged dimers listed in Table 3. In fact, when oxalate bridging is considered, $V_2O_2(OH)_2(C_2O_4)(H_2O)_2$ can be seen to consist of alternating-exchange Heisenberg chains with $S = 1/2$.[24–26] In this case, two exchange constants J and αJ should be considered in order to understand the magnetic properties. However, the value of α is so small that the interaction represented by αJ may be neglected (see Table 3). Therefore, the magnetic data fit very well with the dimeric model.

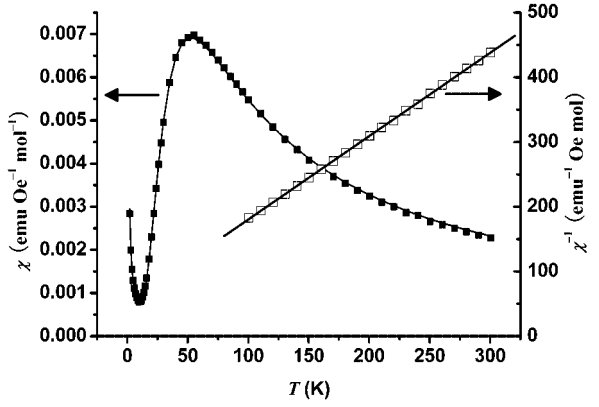

Figure 4. Thermal variation of the molar magnetic susceptibility and the reciprocal magnetic susceptibility for $V_2O_2(OH)_2(C_2O_4)(H_2O)_2$; the solid line represents the best fit obtained with the parameters reported in the text.

Conclusions

The use of oxalate, with the help of H_3BO_3, has led to the preparation of $V_2O_2(OH)_2(C_2O_4)(H_2O)_2$ from V_2O_5. The V_2O_{10} dimer connected by a common edge found in this compound induces a stronger antiferromagnetic coupling than the oxalato-bridged (oxo)vanadium(IV) dimer.[27]

Experimental Section

Materials and Analyses: All reagents were of analytical grade and were used as obtained from commercial sources without further purification. IR spectra were recorded in the 400–4000 cm^{-1} range with a Magna-IR 750 FTIR spectrometer. Elemental analyses were carried out on an Elementar Vario EL III microanalyzer. TG analysis was performed with a heating rate of 10 °C min^{-1} using a Dupont 1090 instrument.

Preparation of $V_2O_2(OH)_2(C_2O_4)(H_2O)_2$ (1): A mixture of V_2O_5 (1.00 g, 5.50 mmol), $H_2C_2O_4{\cdot}2H_2O$ (10.0 g, 79.4 mmol), H_3BO_3 (10.0 g, 162 mmol), and deionized H_2O (15 mL, 0.83 mol) with a mol ratio of about 1.0:14:29:151 was placed in a 50-mL Teflon-lined stainless steel autoclave, and the autoclave was sealed, heated to 155 °C under autogenous pressure for 20 d, and then cooled to room temperature at a rate of 5 °C/h. The pH values of the system before and after synthesis are about 2 and 1, respectively. The blue crystalline product was filtered, washed with hot distilled water, and dried at ambient temperature to give about 1.44 g of complex

Table 1. Single-crystal data and structure refinement details of the compound $V_2O_2(OH)_2(C_2O_4)(H_2O)_2$ (**1**).

Empirical formula	$C_2H_6O_{10}V_2$
Formula mass	291.94
Crystal system	triclinic
Space group	$P\bar{1}$(No.2)
a [Å]	5.2405(10)
b [Å]	5.7340(11)
c [Å]	7.1778(14)
α [°]	76.44(3)
β [°]	69.37(3)
γ [°]	75.37(3)
V [Å]	192.77(8)
Z	1
$\rho_{calcd.}$ [g cm^{-3}]	2.515
μ [mm^{-1}]	2.465
Reflections collected	797
Unique data/parameters	719/61
R_{int}	0.0218
Reflections with $I \geq 2\sigma$	695
Goodness of fit (S)	1.000
R_1/wR_2 ($I \geq 2\sigma$)	0.0472/0.1372
R_1/wR_2 [all data]	0.0483/0.1400

$R_1 = \Sigma(|F_o| - |F_c|)/\Sigma|F_o|$; $wR_2 = [\Sigma w(F_o^2 - F_c^2)^2/\Sigma w(F_o^2)^2]^{1/2}$; $w = 1/[\sigma^2(F_o^2) + (0.1343P)^2 + 0.1200P]$ with $P = (|F_o|^2 + 2|F_c|^2)/3$.

Table 2. Selected bond lengths [Å] and angles [°] for $V_2O_2(OH)_2(C_2O_4)(H_2O)_2$ (**1**).

V1–O5	1.598(3)	O4–V1–O4	79.6(1)
V1–O4	1.993(3)	O4–V1–O3	86.0(1)
V1–O4	2.014(2)	O4–V1–O3	84.8(1)
V1–O1	2.049(3)	O4–V1–O1	160.5(1)
V1–O2	2.059(3)	O4–V1–O1	91.3(1)
V1–O3	2.246(3)	O4–V1–O2	93.6(1)
O1– C1	1.244(5)	O4–V1–O2	164.5(1)
O3– C1	1.250(4)	O2–V1–O3	80.8(1)
C1– C1	1.539(6)	O1–V1–O2	90.8(1)
O5–V1–O4	101.25(1)	O1–V1–O3	75.9(1)
O5–V1–O4	100.70(1)	O3–C1–C1	115.8(4)
O5–V1–O3	171.5(1)	C1–O1–V1	118.8(2)
O5–V1–O1	97.4(1)	O1–C1–O3	127.3(3)
O5–V1–O2	94.2(1)	O1–C1–C1	116.9(4)
V1–O4–V1	100.4(1)	C1–O3–V1	112.5(2)

D–H···A	D···A [Å]	H···A [Å]	D–H···A [Å]
O2–H2A···O4[a]	0.82	1.91	2.714(4)
O2–H2B···O5[b]	0.82	1.93	2.747(4)
O4–H4···O3[c]	0.82	2.00	2.806(3)

[a] Symmetry transformations used to generate equivalent atoms: $-x, -y+2, -z+1$. [b] $x+1, y, z$. [c] $-x+1, -y+1, -z+1$.

Table 3. Best-fit magnetic parameters.

Compound[a]	*g*	*J* [cm^{-1}]	*ρ*	*tip*	*α*
1	1.95 ± 0.01	–29.60 ± 0.05	0.008 ± 0.001	0.00012 ± 0.00001	
1[b]	1.95 ± 0.01	–29.28 ± 0.05	0.002 ± 0.001	0.00004 ± 0.00001	0.025(2)
2[27]	1.93 ± 0.01	–6.50 ± 0.05	0.01 ± 0.002	0.0018 ± 0.00005	
3[27]	1.95 ± 0.01	–6.25 ± 0.05	0.02 ± 0.002	–0.0004 ± 0.00005	
4[18]	1.91	–3.85	0.008		
5[16]	1.927	–4.35		0.00064	

[a] **1**, $V_2O_2(OH)_2(C_2O_4)(H_2O)_2$ (this work); **2**, $[Et_4N]_2[(VO)_2(C_2O_4)_3(H_2O)_2]\cdot 4H_2O$; **3**, $[Et_4N]_2[(VO)_2(C_2O_4)(C_3H_2O_4)_2(H_2O)_2]\cdot 2H_2O$; **4**, $[V_2O_2(C_2O_4)(H_2O)_6]Cl_2\cdot 4Bu_4NCl\cdot H_2O$; **5**, $[Ph_4P]_2[(VO)_2(C_2O_4)_3(H_2O)_2]\cdot 4H_2O$. [b] These values were obtained by fitting the data using Heisenberg alternating chain model with Equation (2) and all others are for the Heisenberg dimer model with Equation (1).

1 (yield 90% based on V_2O_5). Complex **1** is stable and insoluble in water and most organic solvents. $V_2O_2(OH)_2(C_2O_4)(H_2O)_2$ (291.94): calcd. C 8.22, H 2.05; found: C 8.32, H 2.13.

Crystallographic Studies: Intensity data were collected on a Rigaku AFC6S diffractometer with graphite-monochromated Mo-K_α (λ = 0.71073 Å) radiation by using the ω-2θ scan method at room temperature. The structure was solved with direct methods and refined on F^2 with full-matrix least-squares methods using SHELXS-97 and SHELXL-97 programs, respectively.[28] All non-hydrogen atoms were refined anisotropically. The hydrogen atoms were added in the riding model and refined isotropically with O–H = 0.82 Å. The crystallographic data are summarized in Table 1, and the selected bond lengths are listed in Table 2. CCDC-294737 contains the supplementary crystallographic data for this paper. These data can be obtained free of charge from The Cambridge Crystallographic Data Centre via www.ccdc.cam.ac.uk/data_request/cif.

Magnetic Measurements: Magnetic data of polycrystalline samples (H = 5000 Oe) were recorded on 47.90 mg of **1** in the 2–300 K temperature range with a Quantum Design MPMS-5S SQUID Spectrometer. Correction for the sample holder was applied. The data were fitted to the Heisenberg dimer model for two S = 1/2 spins [Equation (1)] whilst taking into account the presence of monomeric paramagnetic impurities (second term) and temperature-independent magnetism (third term) [where χ is the magnetic susceptibility, N_A the Avogadro constant, k_B the Boltzmann constant, μ_B the Bohr magneton, T the temperature, g the g factor, J the exchange constant, ρ the ratio of the paramagnetic impurities, *tip* is the temperature-independent contribution]. The best-fit parameters are given in Table 3.

$$\chi = (1-\rho)\frac{N_A g^2 \mu_B^2}{k_B T}\frac{2\exp\left(\frac{2J}{k_B T}\right)}{1+3\exp\left(\frac{2J}{k_B T}\right)} + \rho\frac{N_A g^2 \mu_B^2}{2k_B T} + tip \qquad (1)$$

The data were also fitted to the Heisenberg alternating chain model with S = 1/2 using the following Equation (2), where the first term describes the Heisenberg alternating chain model, $x = |J|/k_B T$, J is the exchange integral between a spin and its right neighbor, αJ the exchange integral between a spin and its left neighbor, the values for $A(\alpha)$, $B(\alpha)$, $C(\alpha)$, $D(\alpha)$, $E(\alpha)$, and $F(\alpha)$ can be found in ref.[25] The fit was good, and the best-fit parameters are listed in Table 3.

$$\chi = (1-\rho)\frac{N_A g^2 \mu_B^2}{k_B T}\frac{A(\alpha)+[B(\alpha)]x+[C(\alpha)]x^2}{1+[D(\alpha)x+[E(\alpha)]x^2+[F(\alpha)]x^3]} + \rho\frac{N_A g^2 \mu_B^2}{2k_B T} + tip \qquad (2)$$

Acknowledgments

This work was supported by the National Natural Science Foundation of China (Grant 20471003).

[1] G. M. Miskelly, C. R. Clark, J. Simpson, D. A. Buckingham, *Inorg. Chem.* **1983**, *22*, 3237–3241.
[2] J. Carranza, H. Grove, J. Sletten, F. Lloret, M. Julve, P. E. Kruger, C. Eller, D. P. Rillema, *Eur. J. Inorg. Chem.* **2004**, 4836–4848.
[3] H. Oshio, U. Nagashima, *Inorg. Chem.* **1992**, *31*, 3295–3301.
[4] O. R. Evans, W. B. Lin, *Cryst. Growth Des.* **2001**, *1*, 9–11.
[5] U. García-Couceiro, O. Castillo, A. Luque, J. P. García-Terán, G. Beobide, P. Román, *Eur. J. Inorg. Chem.* **2005**, 4280–4290.
[6] E. Coronado, J. R. Galán-Mascarós, C. J. Gómez-García, P. Gütlich, *Chem. Eur. J.* **2000**, *6*, 552.
[7] E. Coronado, J. R. Galán-Mascarós, C. J. Gómez-García, E. Martínez-Ferrero, M. Almeida, J. C. Waerenborgh, *Eur. J. Inorg. Chem.* **2005**, 2064–2070.
[8] S.-H. Yang, G.-B. Li, S.-J. Tian, F.-H. Liao, J.-H. Lin, *J. Solid State Chem.* **2005**, *178*, 3703–3707.
[9] C. N. R. Rao, S. Natarajan, R. Vaidhyanathan, *Angew. Chem. Int. Ed.* **2004**, *43*, 1466.
[10] K. S. Min, A. L. Rhinegold, J. S. Miller, *Inorg. Chem.* **2005**, *44*, 8433–8441.
[11] E. Coronado, J. R. Galán-Mascarós, C. J. Gómez-García, C. Martí-Gastaldo, *Inorg. Chem.* **2005**, *44*, 6197–6202.
[12] H. Tamaki, Z. J. Zhong, N. Matsumoto, S. Kida, M. Koikawa, N. Achiwa, Y. Hashimoto, H. Okawa, *J. Am. Chem. Soc.* **1992**, *114*, 6974–6979.
[13] E. Coronado, J. R. Galán-Mascarós, C. J. Gómez-García, V. Laukhin, *Nature* **2000**, *408*, 447–449.
[14] M. Schindler, F. C. Hawthorne, W. H. Baur, *Chem. Mater.* **2000**, *12*, 1248.
[15] R. Cortes, M. K. Urtiaga, L. Lezama, M. I. Arriortua, T. Rojo, *Inorg. Chem.* **1994**, *33*, 829–832.
[16] O. Costisor, M. Brezeanu, Y. Journaux, K. Mereiter, P. Weinberger, W. Linert, *Eur. J. Inorg. Chem.* **2001**, 2061–2066.
[17] W. M. Chang, S. L. Wang, *Chem. Mater.* **2005**, *17*, 74–80.
[18] S. Triki, F. Bérézovsky, J. S. Pala, M. T. Garland, *Inorg. Chim. Acta* **2000**, *308*, 31–36.
[19] Y. M. Tsai, S. L. Wang, C. H. Huang, K. H. Lii, *Inorg. Chem.* **1999**, *38*, 4183–4187.

[20] W. R. Scheidt, C. Tsai, J. L. Hoard, *J. Am. Chem. SOC.* **1971**, *93*, 3867–3872.
[21] J. Salta, C. J. O'Connor, L. Sichu, J. Zubieta, *Inorg. Chim. Acta* **1996**, *250*, 303–310.
[22] D. B. Leznoff, N. D. Draper, R. J. Batchelor, *Polyhedron* **2003**, *22*, 1735–1743.
[23] M. J. Katz, C. J. Shorrock, R. J. Batchelor, D. B. Leznoff, *Inorg. Chem.* **2006**, *45*, 1757–1765.
[24] J. W. Hall, W. E. Marsh, R. R. Weller, W. E. Hatfield, *Inorg. Chem.* **1981**, *20*, 1033–1037.
[25] W. E. Hatfield, L. W. ter Haar, M. M. Olmstead, W. K. Musker, *Inorg. Chem.* **1986**, *25*, 558–563.
[26] E. Herrling, G. Fischer, S. Matejcek, B. Pilawa, H. Henke, I. Odenwald, W. Wendl, *Phys. Rev. B* **2003**, *67*, 014407.
[27] B. Baruah, V. O. Golub, C. J. O'Connor, A. Chakravorty, *Eur. J. Inorg. Chem.* **2003**, 2299–2303.
[28] a) G. M. Sheldrick, *SHELXS97 Program for Crystal Structure Solution*, University of Göttingen, Göttingen, Germany, **1997**; b) G. M. Sheldrick, *SHELXL97 Program for Crystal Structure Refinement*, University of Göttingen, Göttingen, Germany, **1997**.

Received: February 6, 2006
Published Online: May 18, 2006

